Spectroscopic Studies of Sol−Gel Li/MgO Catalysts

J. L. Boldú,* E. Muñoz, X. Bokhimi, and O. Novaro†

Institute of Physics, National University of Mexico (UNAM) A. P. 20-364, 01000 México D. F., Mexico

T. López and R. Gómez

Department of Chemistry, Universidad Autónoma Metropolitana-Iztapalapa, A. P. 55-534, 09340 México D. F., Mexico

Received October 28, 1997. In Final Form: November 2, 1998

Samples of Li/MgO were generated by co-gelling Li_2CO_3 and $Mg(OEt)_2$, and characterized with the aid of diverse spectroscopic techniques: EPR, FTIR, UV−vis, TGA, DTA, and X-ray powder diffraction (with refinement of the crystalline structure). The presence of the EPR hyperfine structure of Mn^{4+} resulting from the conversion of the unintentionally present impurity Mn^{2+} to Mn^{4+}, establishes clear evidence that lithium ions are present in the sol−gel matrix substituting for magnesium ions. Indeed, only after irradiating the sample with γ rays at liquid nitrogen, the formation of $[Li]^0$ centers in a metastable fashion was possible, but further instability and annihilation occurred when the sample was brought back to room temperature. The sol−gel material described in this work proves to be active in the oxidative coupling of methane.

Introduction

Systems prepared by the sol−gel technique and doped with alkali metals have been extensively studied, especially with lithium as the doping element.[1] Lithium incorporation in the matrix depends on the lithium precursor salt and solvent used for the preparation.[2−4] When alumina and silica are the matrixes, their texture and crystallization depend on the annealing conditions of the gel. For these matrixes, lithium atoms are distributed homogeneously when doping is done by co-gelling a lithium salt and the corresponding matrix alkoxide, but not when it is used as a lithium alkoxide precursor.[3−5] In this latter case, the final product is a mixture of the matrix oxide and lithium oxide.

When different alkaline salts are added to sol−gel silica (with 3% alumina), made from tetraethoxisilane, the alkaline cation easily diffuses into the gel.[6] This can be optimized by using different additives and organic or inorganic lithium precursors.[7]

Gels prepared by the sol−gel technique are different from those prepared by traditional methods. In the sol−gel process, where porosity can be controlled, a large number of OH group ions that are stable at high temperature can be present in the bulk. This produces changes in the physical and chemical properties of the material.

When the materials are fused in lithium salts, M−O−Li bridges are formed. Here, some M−O−M bridges are broken, and lithium ion substitutes for the corresponding cation.[8−10] If the material is prepared using the sol−gel method, the M−O−M bridges are not broken and lithium ions can freely move into the channels interconnected by the gel.[11]

In the present work, MgO gels were prepared by co-gelling magnesium alkoxide with lithium carbonate. It has been reported by several authors,[12−16] that the catalytic activity of Li/MgO catalysts strongly depend on the formation of $[Li]^0$ or F centers.[17]

Our results show that neither $[Li]^0$ nor F centers (paramagnetic or optically active) are strictly necessary for the oxidative coupling of methane, since in our sol−gel preparation such species were not observed either in the EPR present results or in the UV−vis spectra and this not withstanding the resulting materials were to be active in the oxidative coupling of methane.

Experimental Section

Sample Preparation. For the synthesis of sol−gel Li/MgO, a solution with 0.05 mol of $Mg(OEt)_2$, 0.85 mol of ethanol, and 0.02 mol of NH_4OH was prepared. This solution was refluxed at 70 °C under constant stirring. After this mixture was refluxed for 10 min, a Li_2CO_3 aqueous solution was added dropwise into the above solution to reach 1 wt % Li. Refluxing was maintained until a gel was formed, which was dried in air at 70 °C. After synthesis, the fresh sample became a white powder.

Characterization. FTIR. The solid samples were characterized by FTIR spectroscopy with a 170-SX Nicolet spectrometer. A transparent disk was prepared by pressing dried powder.

UV−Visible Spectroscopy. The diffuse reflectance spectra were obtained with a Cary III Varian spectrograph, with

† Member of El Colegio Nacional de México.

(1) López, T.; Gómez; R.; Muñoz, E.; Boldú, J. L.; Novaro, O. *Mater. Lett.* **1994**, *20*, 363.
(2) López, T.; Gómez, R.; Ramírez-Solís, A.; Poulain, E.; Novaro, O. *J. Mol. Catal.* **1994**, *88*, 71.
(3) De Lambilly, H.; Klein, L. C. *J. Non-Cryst. Solids* **1989**, *109*, 69.
(4) Le Bars, N.; Klein, L. C. *J. Non-Cryst. Solids* **1990**, *122*, 291.
(5) Ho, Shu-Fang; Klein, L. C.; Caracciolo, R. *J. Non-Cryst. Solids* **1990**, *120*, 267.
(6) Schwartz, Y.; Anderson, P.; De Lambilly, H.; Klein, L. C. *J. Non-Cryst. Solids* **1986**, *83*, 391.
(7) Wallace, S.; Hench, L. L. *Ceram. Eng. Sci. Proc.* **1984**, *5*, 568.
(8) Charles, R. J. *J. Am. Ceram. Soc.* **1963**, *46*, 235.
(9) Coutaz, J. L.; Jaussand, P. C. *Appl. Opt.* **1982**, *21*, 1063.
(10) Hench, L. L.; Clark, D. *J. Non-Cryst. Solids* **1978**, *28*, 83.
(11) Wakamatsu, H.; Szu, S. P.; Klein, L. C.; Greenblatt M. *J. Non-Cryst. Solids* **1992**, *147−148*, 668.
(12) Wang, Ji-Xiang; Lundsford, J. H. *J. Phys. Chem.* **1986**, *90*, 5883.
(13) Driscoll, D. J.; Martir, W.; Wang, Ji-Xiang; Lundsford, J. H. *J. Am. Chem. Soc.* **1985**, *107*, 58.
(14) Ito, T.; Lundsford, J. H. *Nature* **1985**, *314*, 721.
(15) Ross, J. A.; Korf, S. J.; Veehof, R. H. J.; Van Ommen, J. G.; Ross, R. H. *Appl. Catal.* **1989**, *52*, 131.
(16) Zhen, K.; Li, S.; Bi, Y.; Yang, X. *Catal. Lett.* **1994**, *23*, 369.
(17) Wu, Ming-Cheng; Truong, C. M.; Coutler, K.; Goodman, D. W. *J. Am. Chem. Soc.* **1992**, *114*, 1565.

10.1021/la971173d CCC: $18.00 © 1999 American Chemical Society
Published on Web 12/11/1998

integrating sphere. To obtain the spectra, self-suporting pellets were prepared. The reference was a 100% reflectance sample.

TGA and DTA. Both, DTA and TGA thermoanalysis were performed with a Shimadzu DT-30 apparatus. Both type of measurements were conducted simultaneously from room temperature to 1000 °C at a heating rate of 20 °C/min.

X-ray Diffraction. The crystalline structure of the phases in the sample was characterized by X-ray powder diffraction and refined by the Rietveld method. X-ray diffraction patterns were measured at room temperature with a Siemens D-5000 diffractometer having Cu Kα radiation, and a graphite secondary beam monochromator. Specimens were prepared by packing sample powder in a glass holder. Intensity was measured by step scanning in the 2θ range between 20 and 130°, with a step of 0.02° and a measuring time of 2 s per point. Crystalline structures were refined by using DBWS-9411[18] and WYRET[19] software. Peak profiles were modeled by taking into account its broadening produced by crystallite size and microstrain.[20,21] The standard deviations, showing the variation of the last figures of the corresponding number, were given in parentheses. When the numbers correspond to parameters obtained from the Rietveld refinement, the estimated standard deviations are not estimates of the analysis as a whole, but only of the minimum possible probable errors based on their normal distribution.[21] From the refinement of the crystalline structures in the sample, the obtained lithium concentration corresponded to its nominal composition of 1 wt %.

EPR. Electron paramagnetic resonance (EPR) measurements were performed on a JEOL JES-RE3X spectrometer, using a cylindrical cavity (TE_{011} mode) with 100 kHz field modulation. *g* values were obtained by measuring the resonance field with an NMR gaussmeter ES-FC5 (JEOL), while the operating frequency was measured with a counter HP-5350B. For the low-temperature measurements, a DVT2 (JEOL) variable-temperature controller unit was employed. All EPR spectra were recorded at −163 °C.

Results and Discussion

FTIR. Magnesia is known to be a relatively inert oxide, especially when it has been thermally treated at temperatures above 800 °C. However, when magnesia is prepared via an alkoxide route, it preserves several −Mg−OH− groups at temperatures approaching 600 °C.[22] The infrared vibrations associated with these groups are present in the 4000−3000 cm^{-1} range.

In the fresh sample, the observed sharp and intense stretching vibration band at 3698 cm^{-1} is attributed to the existence of −Mg−OH− bonds (Figure 1a). Another band at 3644 cm^{-1} is also associated with stretching vibrations of the OH groups.

The presence of lithium carbonate in the magnesia sol creates oxalates that are responsible for the intense bands at 1646 and 1671 cm^{-1}, which are connected with the bending vibration of the carbonyl group, and the typical band of OH flexion vibrations arising from residual water shows at 1630 cm^{-1}. Stretching C−O bands due to carbonates in the solid are present at 1700 and 840 cm^{-1}, although part of the carbonate was transformed into oxalates and another part remains as Li_2CO_3 totally dispersed in the magnesia. The band at 1570 cm^{-1} (present only in the fresh sample case), attributed to a scissors type vibration of the C−H residual organic groups, totally disappears at higher temperatures when the OBut (butoxy) groups are desorbed.

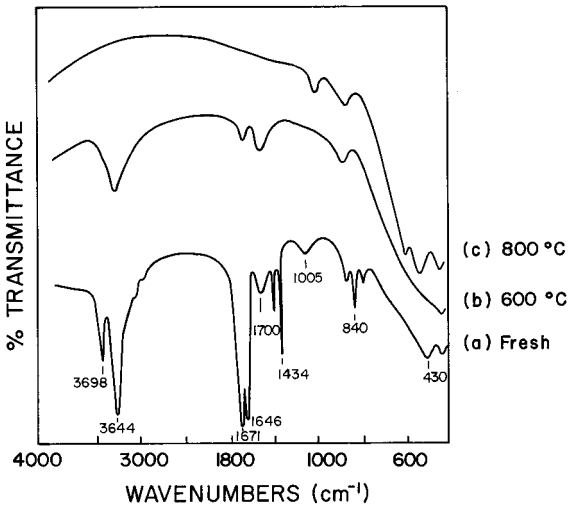

Figure 1. FTIR spectra of sol−gel Li/MgO sample.

Bands shown at 1005 and 430 cm^{-1} were produced by the bending vibrations of the Mg−O bonding in magnesia. Since lithium atoms are very light, any vibrations related to their bonds could not be observed in the spectrum. The lithium incorporated in the lattice, however, provoked shifts in the absorption bands of pure magnesia.[23]

When the sample is thermally treated at 600 °C, the previously observed 3698 cm^{-1} peak disappears, and the one at 3644 cm^{-1} reduces its intensity, since the dehydroxylation process is taking place. The bands at 430 and 1005 cm^{-1} are not clearly resolved, most probably due to the remnant oxalates still present in the material at this temperature that hinder and disperse such absorption frequencies. Similarly, the intensity of the 1646 cm^{-1} peak decreases significantly.

As shown ahead in the DTA, TGA, and XRD results, the oxalate group decomposes around 380 °C releasing CO_2; therefore, the bands associated with the C=O bond are not present in the FTIR of the sample treated at 600 °C (Figure 1b), but the carbonate has been only partially desorbed as noticed in the correspondent bands as well as their shift to higher energies.[23]

The typical Mg−O bands of magnesia (periclase) are again observed (Figure 1c) when the sample is treated at 800 °C, and the bands associated with hydroxyls and oxalates are not present in the high energy regime.

UV−Visible Optical Absorption. Attempts to obtain optical absorption signals were unfruitful for samples incubated at temperatures from 200 °C up to 800 °C. Therefore, it was not possible to detect absorptions in the UV portion at 254 nm (5.0 eV), where the charged oxygen vacancies (F or F^+ centers) are normally present, nor in the visible region where the $[Li]^0$ optically responds, which had been unequivocally identified at 690 nm (1.8 eV).[24]

DTA and TGA. Samples showed an endothermic reaction at 100 °C (Figure 2a) produced by evaporation of both residual water and residual ethanol, as well as the dehydroxylation of glushinskite. A sample weight loss of 0.9% of its initial weight was associated with this reaction (Figure 2b). At 380 °C, the sample had a second endothermic reaction caused by the partial dehydroxylation of brucite and the magnesium oxalate decomposition. A sample weight loss of 14.9% was associated with this reaction. Finally, when the sample was heated at

(18) Young, R. A.; Sakthivel, A.; Moss, T. S.; Paiva-Santos, C. O. *J. Appl. Crystallogr.* **1995**, *28*, 366.
(19) Schneider, Margarita. EDV-Vertrieb, Starnbergweg 18, D-8134 Pöcking, Germany. Telephone: 0049-8157-8727. Fax: 0049-8157-4527. Personal communication, 1992.
(20) Thompson, P.; Cox, D. E.; Hastings, J. B. *J. Appl. Crystallogr.* **1987**, *20*, 79.
(21) Prince, E. *J. Appl. Crystallogr.* **1981**, *14*, 157.
(22) López, T.; García, Y.; Gómez, R. *J. Catal.* **1991**, *127*, 75.
(23) Nakamoto, K. *Infrared and Raman Spectra of Inorganic and Coordination Componds*; 3rd ed.; Wiley: New York, 1977.
(24) Lacy, J. B.; Abraham, M. M.; Boldu, J. L.; Chen, Y.; Narayan, J.; Tohver, H. T. *Phys. Rev. B* **1978**, *18*, 4136.

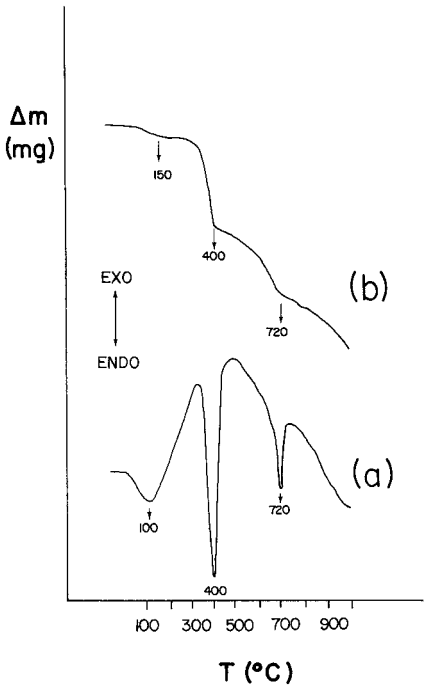

Figure 2. DTA (a) and TGA (b) curves of a typical Li/MgO sample. They were taken at an annealing rate of 20 °C/min.

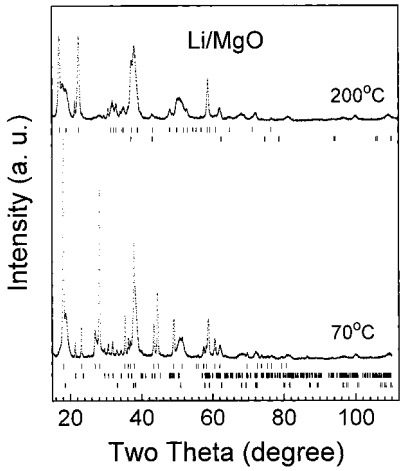

Figure 3. X-ray diffraction patterns of the fresh sample (70 °C) and of the sample after its annealing at 200 °C. The tick marks in the low part of the figure correspond to glushinskite (upper tick marks), lithium carbonate (middle tick marks), and brucite (lower tick marks). The tick marks in the middle of the figure correspond to dehydrated magnesium oxalate (upper tick marks) and periclase (lower tick marks).

around 700 °C, lithium carbonate was decomposed, releasing carbonyl groups and producing an additional sample weight loss of 12.5%.

X-ray Diffraction. The fresh sample exhibited three crystalline phases (Figure 3a): glushinskite ($MgC_2O_4 \cdot 2H_2O$), lithium carbonate, Li_2CO_3, and brucite, $Mg(OH)_2$. Since Li atoms scatter X-rays weaker than magnesium atoms, the diffraction pattern of glushinskite, which is a hydrated magnesium oxalate,[25] dominated the diffraction pattern. This does not mean however, that glushinskite was the majority phase. Phase concentrations can only be determined after refinment of the crystalline structure of all phases in the sample. The atom positions for the Glushinskite unit cell, however, were not available;

(25) Levy, Walter L.; Perrotey, J.; Visser, J. W. *Bull. Soc. Chim. Fr.* **1971**, 757.

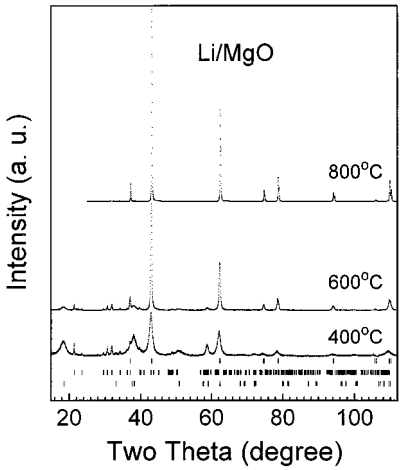

Figure 4. X-ray diffraction patterns after annealing the sample at 400, 600, and 800 °C. Upper tick marks correspond to periclase, middle tick marks to lithium carbonate, and lower tick marks to brucite.

Table 1. Concentrations and Average Crystallite Sizes of Brucite and Periclase as a Function of Temperature

	periclase		brucite	
T (°C)	concentration (wt %)	av crystallite size (nm)	concentration (wt %)	av crystallite size (nm)
400	64	9.2 (5)	36	4.4 (1)
600	89	40.0 (9)	11	4.4 (1)
800	100	138 (2)	0	

therefore, its crystalline structure was not refined, and a quantitative analysis for the fresh sample was impossible.

When the sample was annealed at 200 °C, glushinskite was partially dehydrated and transformed into dehydrated magnesium oxalate (MgC_2O_4), which coexisted in the sample with glushinskite, lithium carbonate, brucite, and a small amount of periclase (MgO) that was produced by the initial dehydratation of brucite. At this temperature lithium carbonate did not suffer any transformation.

After the sample was annealed at 400 °C, the magnesium oxalates disappeared, and about half of the brucite was dehydrated and transformed into periclase (Table 1). Brucite and periclase were nanocrystalline with average crystallite sizes smaller than 10 nm (Table 1, and Figure 4). Lithium carbonate was still present in the sample in a concentration that was constant even after annealing the sample at 600 °C. After annealing the sample at this temperature, periclase was the main phase (Table 1, and Figure 4), with an average crystallite size of 41 (1) nm. Brucite's average crystallite size did not change.

The crystalline structure of periclase was refined with a cubic unit cell with the symmetry described by space group $Fm3m$, brucite's structure with a trigonal unit cell with the symmetry described by space group $P\bar{3}m1$, and lithium carbonate's structure with a monoclinic unit cell with the symmetry described by space group $C2/c$.

When the sample was annealed at 800 °C, periclase with an average crystallite size of 138 (2) nm was the only phase in the sample, while lithium carbonate disappeared.

EPR. Prior to EPR experiments, the fresh sol−gel Li/MgO powders were dried in air for 2 h at 200 °C and immediately placed in the fused quartz sample tube, which was introduced into the EPR cavity. Spectra were obtained by sweeping the static magnetic field while recording the first derivative of the absorption spectrum.

EPR spectra were obtained after different heat treatments of the sample (Figure 5). It is worth mentioning that all the EPR traces showed iron, chromium, and

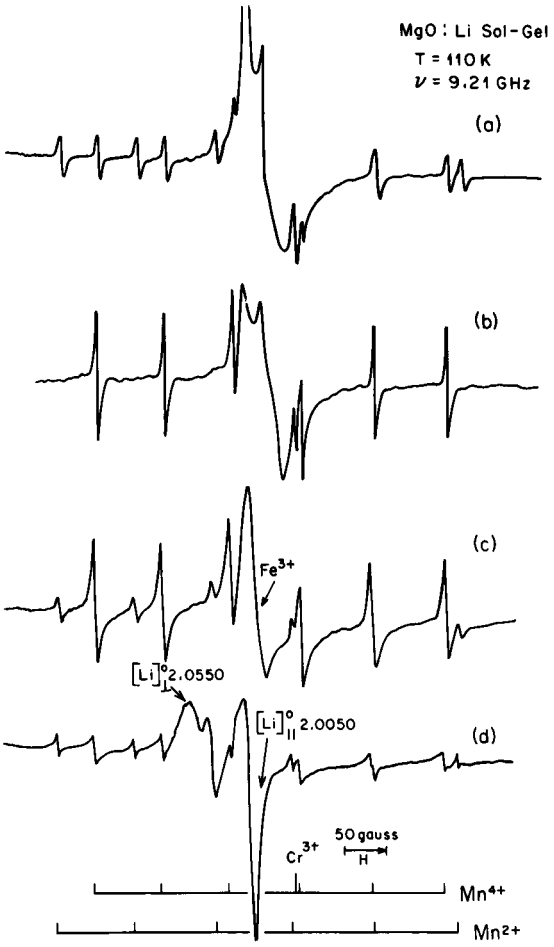

Figure 5. EPR spectra of sol−gel Li/MgO samples measured at X-band (9.2 GHz) and at temperature of −163 °C: (a) sample without any special heat treatment; (b) sample heated at 1000 °C for 7 min in flowing O_2; (c) sample γ-irradiated (1 MRad) at room temperature; (d) sample γ-irradiated (1 MRad) at liquid-nitrogen temperature. Here, the presence of $[Li]^0$ centers is evident.

manganese, as unintentional impurities in the MgO matrix. Due to their paramagnetic nature, they were distinctly detected by EPR spectroscopy. Figure 5a shows the spectrum for a dried Li/MgO sample. The corresponding EPR spectrum, obtained at −163 °C, exhibited the coexistence of divalent and tetravalent manganese ions along with Cr^{3+} and that corresponding to the Fe^{3+} central fine transition at the very center of the spectrum. The tetravalent manganese ions detected in this spectrum were produced by the presence of lithium ions and Mg vacancies in MgO lattice.[26,27] $[Li]^0$ centers were not detected in this sample.

Figure 5b corresponds to a sample oxidized at 1000 °C in flowing O_2 for 7 min. The trace showed mainly the six Mn^{4+} hyperfine set resulting from the conversion of Mn^{2+} to Mn^{4+}. Mn^{2+} EPR transitions were absent, but the amount of Mn^{4+} considerably increased, suggesting that more Li^+ ions were incorporated into the MgO lattice.

The EPR spectrum of the sample exposed to irradiation (1 Mrad) at room temperature with γ-rays (Figure 5c) did not show any change. As expected, no $[Li]^0$ centers were detected in the sample.

The sample, cooled at liquid-nitrogen temperature, was further irradiated with γ-rays (1 Mrad) and maintained at that temperature until its insertion into the microwave cavity for EPR observation. After this sample treatment, the presence of new absorption lines in the spectrum was evident (Figure 5d). These new contributions clearly indicated the presence of axial $[Li]^0$ centers with their perpendicular ($g = 2.055$) and parallel ($g = 2.0050$) contributions.[27] At X-band frequencies the parallel contribution was partially masked due to its superposition with the central fine structure line of the strong Fe^{3+} signal.

The irradiated sample was warmed-up "in situ" in the microwave chamber, at steps of 20 °C until the signals arising from the contribution of lithium centers were completely annihilated near 0 °C. During the warming-up process, both contributions of the axial $[Li]^0$ centers approached each other until they became a single line, as expected.[27] This new integrated signal was found at the average magnetic field position corresponding to $g_{av} = 2.038$, which agreed with previous observed results.[26] Further attempts to recover the $[Li]^0$ signals by cooling the sample back to liquid-nitrogen temperature were unsuccessful, indicating that the lithium centers formed by γ-ray irradiation were the product of a metastable state. After irradiation the sample presented the characteristic bluish coloration that disappeared during the warm-up procedure.

Specific Area. The specific BET surface area of the studied sample resulting from the N_2 adsorption isotherm systematically decreases as the thermal treatment proceeds. Indeed, samples treated in air for 4 h exhibit BET areas of 70, 40, 31, and 15 m^2/g when incubating temperatures were 200, 400, 600, and 800 °C, respectively.

Catalytic Activity. Preliminary results of the catalytic activity in the oxidative coupling of methane (CH_4:O_2 = 1:1 in helium flow) for the Li/MgO sol−gel sample after 3 h on stream at 750 °C showed conversions of 49% mol and selectivities of 9.0, 51.9 and 38.9% mol for CO, CO_2, and ethane, respectively. The evolution of the catalysts and the interpretation of the behavior regarding the acidity and selectivity are experiences currently in course. They will be a matter for a future extended work.

Conclusions

When Li/MgO catalysts were prepared by using a sol−gel method with Li_2CO_3 and $Mg(OEt)_2$, Li^+ ions may be incorporated into the MgO lattice starting at 150 °C. Even for small lithium doping concentrations, EPR spectra are significantly affected, indicating that EPR spectroscopy is ideal for analyzing the behavior of lithium ions in the MgO lattice.

The presence of Li^+ ions in the MgO lattice was evident by the appearance of the six Mn^{4+} hyperfine set resulting from the conversion of Mn^{2+} to Mn^{4+}, produced by the required charge compensation of the lithium substituting for magnesium ions. The presence of lithium ions in magnesium sites creates active centers for the oxidative coupling of methane, since the preliminary results of the activity for the sol−gel preparation showed that such catalysts were active in the mentioned reaction, without the necessity of the presence of either $[Li]^0$ or F centers.

Acknowledgment. We would like to thank Mr. A. Morales, Mr. J. Barreto, and Mr. A. Sánchez for technical support and to the CONACyT (Mexico), the CNRS (France), and the NSF for financial support.

LA971173D

(26) Davies, J. J.; Smith, S. R. P.; Wertz, X. *Phys. Rev.* **1969**, *178*, 608.

(27) Abraham, M. M.; Chen, Y.; Boatner, L. A.; Reynolds, R. W. *Phys. Rev. Lett.* **1976**, *37*, 849.